EUROPEAN SYNCHROTRON RADIATION FACILITY

INSTALLATION EUROPEENNE DE RAYONNEMENT SYNCHROTRON

ESRF

Long Term Project Report : Interim/Final

Summary Page

Proposal Number: MX1510

1. Beamtime Used

Please give a short summary of progress for each scheduling period for which beamtime has been allocated/used :

Scheduling period	Beamline(s) Used	Shifts Used	Summary of results obtained
2013 /II	BM29	18 (2 x 9)	**Proof of concept**: design of pod adapted to BM29 including a thin capillary, connected to a microfluidic chip ; test of material (glass and kapton) for SAXS signal; successful generation of droplets in capillary Next run on 1rst March (postponed 14th april)
2014 /I	BM29	18 (2 x 9)	**Validation of the experimental set-up**: Choice and test of material (protein, oil, surfactant) that does not present radiation damage. Rasburicase in droplets behave as in usual solution.
2014 /II	BM29	18 (2 x 9)	**Study of phase transition** of glucose isomerase. Crystals appear in droplets and good quality SAXS signals are obtained **Study of weak interactions** of lysozyme. SAXS signal for different lysozyme and salt concentrations are obtained. Second virial coefficient of lysozyme as a function of salt concentration is obtained.
2015 /I	BM29	18 (2 x 9)	Improvement of the experimental set-up. Protein interaction in solution measurements. First trial to measure nucleation
2015 /II	BM29	18 (2 x 9)	Improvement and development of the synchronization between droplets, shutter and acquisition of SAXS data Observation of pre-nucleation clusters.
2016 /I	BM29	9 (1 x 9)	Implementation of on-line (i.e. on chip concentration measurements) using UV light and spectrometer Observation of pre-nucleation clusters (possibly internal structure).

2. Resources Provided by User team (financial, personnel, technical...):

Two other research projects were submitted at the same time in 2013 (DEFI MI CNRS and ANR JCJC) for coupling this microfluidic chip to SAXS experiment at ERSF. These two projects allowed us to buy a pinhole for BM29 (8000€), technical for microfluidics at Toulouse and chromatography column at Avignon to prepare proteins. The ANR JCJC, long term project 2014-2016, has begun in February 2014, and permitted the recruitment of a PhD student allocated to this project since March 2014

(Dimitri Radajewski); it will also allow us to have 2 Master students (one in 2016 and one in2017). We also recruited an undergraduate student (Robin Lescure June - July 2015) to help us for microfabrication and for experiments performed at ESRF. Some essential equipment's such as 4 microfluidic pumps or synchronization equipment (camera, oscilloscope and delay generator) are carried from LGC Toulouse to ESRF for each run and the chip are especially designed at the LGC Toulouse. From a technical point of view, we have developed a robust set-up (based on real time image analysis) to synchronize the droplets and the shutter and the detector (further details on the set-up will be given in the report). This setup allows to get a better resolution at low angle and to expose only the inside of the droplets (without shooting the droplet interface or the oil).

In addition, during the last year of the LTP project, LGC has recruited a post doc specialist of photonic lab-on-chip allowing us to implement on chip concentration measurements (in the UV-vis range). More details are given in the report.

At the end, of the project, we (LGC IBMM and BM29 members) have developed robust microfluidic platforms allowing to precisely control temperature in the range of 40°C to 0°C (from the generation of the droplets to the SAXS sample chamber), to mix on chip samples (no preparation needed) , to analyze sample from 30 sec to few hours after mixing (for kinetics studies) , to measure protein concentration inside the generated droplets (with a precision of few nanomolar and for concentration ranging from 0.1mg/ml to 90mg/ml – depending of the optical path) and to acquire unambiguous SAXS (and "easy" to treat) data thanks to the developed real time image analysis software. All the chips, software, and concept developed during these 3 years of collaboration are of course available for ESRF (we can freely build chips for ESRF, and reproduce freely the housing of chips and experimental setup for the beamline).

3. **Technical and Scientific Milestones Achieved** (in relation to the milestones identified in the original proposal)**:**

Year 1

Objectives: Technological developments – Chip & Pod design and testing.

2013/II: The LTP has begun in October 2013. 3 pods adapted to the beamline BM29 have been built either with glass capillary (with and without hydrophobic surface coating) or kapton capillary. These PODS have been used to test different microfluidic chip configurations; the first one tested generated moving droplets.
The remaining shifts (12) of this year 1 have been dedicated to the introduction of the microfluidic chips in the POD, the stability of the protein in droplets and the acquisition of crystallographic structure of a model protein (glucose isomerase).
2014/I: During the 6 first shifts, in April 2014, different carrier oils, surfactants for generating droplets of proteins or buffers from the microfluidic chip have been tested for radiation damage and background signal. In the case where no radiation damage was observed, buffer signal and protein signal could be measured in static and moving droplets. Rasburicase has been used as a model protein and the good combination of material (oil, surfactant) has been found to avoid radiation damage and have a signal of the protein corresponding to the signal obtained from atomic coordinate.

Deliverables of the first year (Microfluidic chips compatible with SAXS measurements) have been obtained and objectives (Design, development and test of the chips needed in task of year 2 and 3) have been achieved.

Year 2

Objectives : Phase diagram of macromolecules and crystallization experiments.

Year 2: 2014/II: In the 6 following shifts, another protein, glucose isomerase has been tested in the same conditions (oil, surfactant) as Rasburicase. A crystallization agent (polymer) was added. Some crystals appeared in the droplets just after the generation, suggesting a phase transition occurred. SAXS signals of protein have been obtained and diffraction peaks could be related to the crystallographic structure of the protein. In the last 6 shifts of 2014, in November, lysozyme has been used as a model protein. Same conditions were used with NaCl as a crystallization agent. This time no crystallization occurred but it was possible to study the weak interactions of protein in solution as a function of salt concentration. SAXS signals for different lysozyme and salt concentrations were quickly obtained and with a small quantity of protein. The different SAXS signals were studied to have access to the second virial coefficient variations as a function of salt, and thus to the phase diagram of lysozyme.

50% of the objectives and deliverables of the second year has been obtained since it has been possible to obtain information on protein structure and interactions in solution.

Rest of the year has been dedicated to the second objective: nuclei size distribution during nucleation.

2015/I: To attain the objective of measuring nucleation cluster a better experimental setup was needed. Consequently, the main purpose of the run was to improve the synchronization between the droplets and the X ray Beam, in order to avoid any measurement artefact from the oil or from the droplet interface (the setup is detailed in the report). During this run, we modify the chip design in order to first generate and store the droplets at a temperature higher than the solubility of the protein in the solution (to avoid any unwanted nucleation) and the system is quickly cooled down to room temperature to induce nucleation. The droplets are then send to the exposure unit of BM29. Using this set-up, we were able to measure the formation of large aggregates (see the low angle signal in the SAXS curves). However, the design of the chip and the distance between the chip and the sample chamber is too high and we observe nucleation and phase transition inside the chip which induce clogging of the chip. During this run we do not have time to test the other chips.

2015/II

Year 3

Objectives : Nucleation experiments at different time-scales

2015/II During the first run (in July 2015) we have experienced a lot of technical problem during the synchronization between the droplets and the beam. Even with the help of the beamline scientists, engineers and technicians, it was difficult to find the origin of the problem (shutter or informatics problem). We spent most of the beamtime to solve the problem and no scientific results could be obtained.

For the second run (in October 2015), we still have some synchronization due to opening and closing time of the shutter, we spent half of the shift to solve the problem, but we never find the good solution. So we decided to operate the synchronization without the shutter. During this run, we were

able to measure few hundreds of supersaturated droplets. It appears clearly that some droplets contain nucleation clusters before the formation of the crystal (see fig. 7in the report).

During this year, we improve the experimental set-up for measuring crystallization, protein – protein interactions and we are ready to measure nucleation of protein inside droplets. However, due to a lot of unexpected technical and experimental problems, only 75% of the objectives were attained since we were only able to "observe qualitatively" nucleation because all the scheduled experiments could not be performed.

2016/I During this run, we were able to measure the formation of cluster formation prior to the appearance of the crystal in the solution. To do so, the experimental setup has been modified in order to perfectly control temperature from the droplet generation until the SAXS sample chamber. In addition, to be sure of the protein concentration used, we also have implemented an on-line concentration measurement using UV spectrometry. The results obtained show that for low protein concentration no cluster (or correlation length were observe). However at high protein concentration the different behaviour of scattering curves were obtained, which is a signature of the modification of the solution structure. Unfortunately, due to the short sample to detector distance of the beam line, the Guinier region of the aggregates were not obtained, giving thus an incomplete information of the cluster formation process (for information, these experiments have been repeated in another beamline with a larger detector distance, the results have shown that at lower q, the same structure factor was obtained, however, we observed a Guinier plateau around 0.08nm^{-1} corresponding to aggregates size around 60 to 80nm).

The objectives of this year have been partially fulfilled; we were able to detect and to observe the formation of pre-nucleation clusters. To interpret the results Monte-Carlo simulation has been initiated and the work is still ongoing.

4. List of publications directly resulting from beamtime used for this Long Term Project:

Publication in Peer Review journals:

Coupling High Throughput Microfluidics and Small-Angle X-ray Scattering to Study Protein Crystallization from Solution Nhat Pham, Dimitri Radajewski, Adam Round, Martha Brennich, Petra Pernot, Béatrice Biscans, Françoise Bonneté, and Sébastien Teychené *Analytical Chemistry* **2017** *89* (4), 2282-2287 DOI: 10.1021/acs.analchem.6b03492 (IF 5.886)

Photonic lab on a chip sensors coupled to innovative high-throughput SAXS approaches for macromolecular studies Isaac Rodríguez-Ruiz, Dimitri Radajewski, Nhat Van Pham, Sophie Charton, Martha Brennich, Petra Pernot , Francoise Bonneté and Sébastien Teychené, 2017 *Submitted* ***upon invitation to Sensor*** (IF 2.8)

Crystallisation in situ - and much more - at the ESRF BioSAXS BM29 beamline Petra Pernot, Françoise Bonneté, Sébastien Teychené Nhat Pham, Dimitri Radajewski, Béatrice Biscans, Martha Brennich and Adam Round Acta Crystallographica Section A: Foundations and Advances 71(a1)

Communications in international congress:

Coupling Small Angle X-ray Scattering and droplet microfluidics towards in-situ observation of pre-nucleation clusters D. Radajewski, I. Rodríguez- Ruiz, T. Bizien, B. Biscans, F. Bonneté, S. Teychené, ISIC 20, Dublin Sept 2017

Coupling microfluidics and Small-Angle X-ray scattering to study the whole crystallization process of proteins in solution Dimitri Radajewski, Isaac Rodriguez Ruiz, Nhat Pham, Thomas Bizien, Martha

Brennich, Petra Pernot, Béatrice Biscans, Françoise Bonneté, and Sébastien Teychené, 24 congress of IUCR, Hideradad, India, August 2017.

Coupling digital microfluidics and Small-Angle X-ray scattering : toward a better understanding of nucleation D. Radajewski, M. E. Brennich, A. Round, P. Pernot, B. Biscans, F. Bonneté, S. Teychené, CGOM 2016 Leeds, UK.

Coupling Droplet Microfluidic and Small Angle X-Ray Scattering N. V. Pham, D. Radajewski, P. Guillet, M. E. Brennich, A. Round, P. Pernot, B. Biscans, F. Bonneté, S. Teychené 19th International Symposium on Industrial Crystallization – 2014 - Toulouse France

Coupling droplet microfluidic and small angle X-ray scattering: Toward on-line measurement of first nucleation step , D. Radajewski, N. V. Pham, P. Guillet, M. E. Brennich, A. Round, P. Pernot, B. Biscans, F. Bonneté, S. Teychené 15th International Conference on the Crystallization of Biological Macromolecules – 2014 Hambourg- Germany

Coupling digital microfluidics and Small-Angle X-ray scattering to study the whole crystallization process of proteins in solution S. Teychené, D. Radajewski, N. V. Pham, A. Round, M. Brennich, P. Pernot, B. Biscans, F. Bonneté. USER MEETING ESRF 2014 (invited)

Coupling digital microfluidics and Small-Angle X-ray scattering D. Radajewski, P. Guillet, M. E. Brennich, A. Round, P. Pernot, B. Biscans, F. Bonneté, S. Teychené, EMBL Conference: Microfluidics 2014 – Heidelberg

Communications in national (French) congresses:

Suivi de la cristallisation de proteins : couplage microfluidique et diffusion de rayons X aux petits angles. Dimitri Radajewski, Isaac Rodriguez Ruiz, Nhat Pham, Martha Brennich, Petra Pernot, Béatrice Biscans, Françoise Bonneté, and Sébastien Teychené, Proceeding of Cristal 8 Rouen 2016.

Coupling digital microfluidics and Small-Angle X-ray scattering to study the whole crystallization process of proteins in solution S. Teychené, D. Radajewski, N. V. Pham, A. Round, M. Brennich, P. Pernot, B. Biscans, F. Bonneté. Journée Cristech Autrans 2014

Coupling digital microfluidics and Small-Angle X-ray scattering to study the whole crystallization process of proteins in solution S. Teychene´, D. Radajewski, N. V. Pham, A. Round, M. Brennich, P. Pernot, B. Biscans, F. Bonnete´. Journée Scientifique C'nano Porquerolles 2014 (Inivted)

REPORT FINAL: LTP MX-1510 on Beamline BioSAXS BM29

Proposal title: **Coupling Droplet Microfluidic and SAXS for mapping protein phase diagrams**

Authors

Dr. Petra Pernot
Dr. Francoise Bonnete
Dr Adam Round
Sebastien Teychene
M. Van nhat Pham
M. Emmanuel Cid
Dr Beatrice Biscans
Martha Brennich

Experimental Session

Beamline	Allocated shifts	Start Date	Finish Date	Local Contact
BM29	9	27 nov. 2013	28 nov. 2013	Petra Pernot (email: rejma@esrf.fr)
BM29	9	31 oct. 2013	01 nov. 2013	Petra Pernot (email: rejma@esrf.fr)
BM29	9	not decided yet	not decided yet	
BM29	9	12 juin 2014	14 juin 2014	Petra Pernot (email: rejma@esrf.fr)
BM29	9	13 avr. 2014	15 avr. 2014	Matthew Bowler (email: mbowler@embl.fr) Petra Pernot (email: rejma@esrf.fr)
BM29	9	27 févr. 2015	01 mars 2015	Petra Pernot (email: rejma@esrf.fr)
BM29	9	13 nov. 2014	15 nov. 2014	Barbara Calisto machado (email: barbara.calisto@esrf.fr)
BM29	9	09 juil. 2015	11 juil. 2015	Petra Pernot (email: rejma@esrf.fr)
BM29	9	09 oct. 2015	11 oct. 2015	Petra Pernot (email: rejma@esrf.fr) Martha Brennich (email: brennich@embl.fr)
BM29	9	08 juil. 2016	09 juil. 2016	Petra Pernot (email: rejma@esrf.fr)
BM29	9	23 avr. 2016	25 avr. 2016	Martha Brennich (email: brennich@embl.fr)
BM29	9	07 juil. 2016	08 juil. 2016	Susana Goncalves (email: sgoncalv@esrf.fr)
BM29	9	not decided yet	not decided yet	
BM29	0			
BM29	0			

Objectives of the project:

Up to now, no experimental technology makes in-situ measurements of size and shape of nuclei during the crystallization process possible, while understanding this step is essential in numerous fields such as biology, chemistry, pharmaceutics, etc.). In a crystallization experiment, two phenomena occur, nucleation and growth, which are generally difficult to dissociate. It has long been known from theory that by decreasing crystallization volumes, crystal growth is slowed down, which could make nucleation observable.

This is in this context that we have proposed to couple microfluidic, in which nanosized droplets are generated, with SAXS experiments in order to measure size and shape of nuclei in different timescales from µsec to min with different samples in various physico-chemical conditions.

In this project, we have developed several microfluidic platforms adapted to measure form factors, structure factor, proteins-proteins interactions in solution, crystal growth and nucleation precursors. The developed platforms allows to generate monodisperse droplets (with well controlled size), at a

precise temperature (ranging from 0°C to 40°C) to measure online concentration (by coupling fiber optics, light source and spectrometer on chip), and to get unambiguous SAXS data (thanks to a synchronization protocol between the droplets and the X ray beam). For kinetic studies different droplet residence time can be achieved ranging from 30s to few hours.
Originally, this project aim to gather information about nucleation mechanism, but the tools developed here are rather generic, easy to use and to interface in BSXcube, and can be applied to other BioSAXS experiments (i.e. protein folding and unfolding, protein aggregation for instance,).

The first year 1 was dedicated to technological developments – Chip & Pod design and testing.
Objectives: *Design, development and test of microfluidic chips needed in tasks of year 2 and 3 in the project*
A good combination of compounds (oil: Krytox GPL100, surfactant: PFPE-PEG-PFPE) has been determined and the SAXS signal of a protein (urate oxidase) in droplets is the same as the signal obtained from the atomic coordinate meaning that **the objectives of the first year** (*Design, development and test of the chips needed in task of year 2 and 3, Microfluidic chips compatible with SAXS measurements*) **have been achieved**.

The first year 1 is dedicated to technological developments – Chip & Pod design and testing.
Objectives: *Design, development and test of microfluidic chips needed in tasks of year 2 and 3 in the project*

A first design for microfluidic chip has been built at the LGC Toulouse for the proof of concept and is described below.

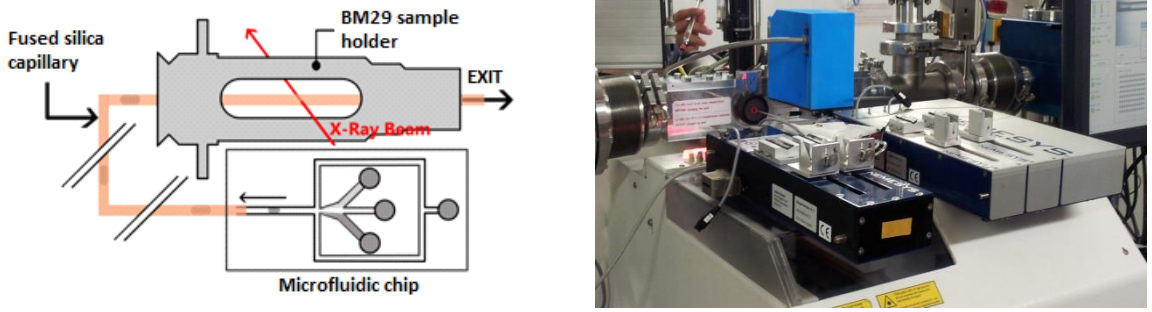

Figure 1- schematic design of chip connected to BM 29 pod (left) ; 4 syringe pumps are connected to chip to generate circulating droplets of aqueous solution in continuous circulating oil (right)

This device was tested during the first two runs. The dimensions of the capillary (250µm x 250 µm) were adapted to the X-ray beam. However the materials used, glass and kapton, give different background signal when empty and filled with water (figure 2).

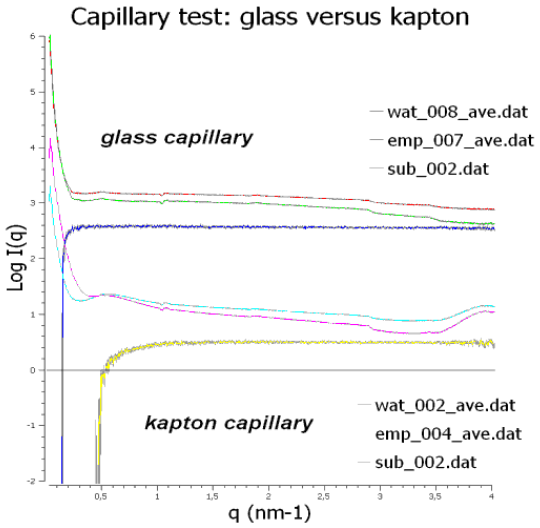

Figure 2- SAXS of an empty capillary or filled with water : glass capillary and kapton capillary

A standard protein, BSA (bovin serum albumin), was tested with success in the glass capillary without oil in static for scattering/absorption ratio. However first tests performed with moving droplets of BSA generated by an usual perfluorinated oil (FC40) show radiation damages either by deterioration of oil or of glass surface coating. Different surface coating, oils surfactants and capillaries were therefore tested. Even though kapton does not appear as the best material when empty or filled with water (figure 2), droplets of urate oxidase generated with FC77 oil gave encouraging results (Figure 3) at middle angles. However at very small angles, aggregation appears and at large angles residual signal of kapton appears.

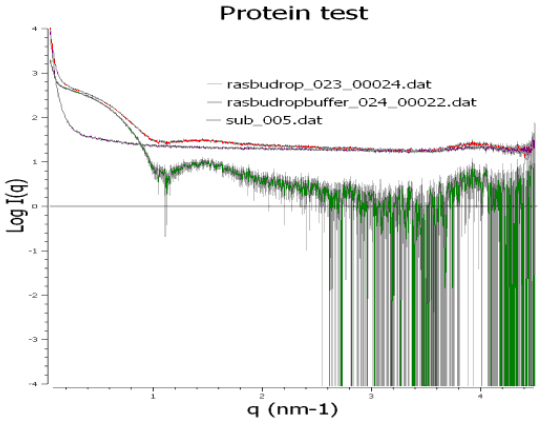

Figure 3- SAXS signal of urate oxidase and its buffer in kapton capillary

In order to use glass capillary in which SAXS signal is better, radiation resistant perfluorinated oil (Krytox 100, Dupont or Perfluorodecalin) has been tested. The quartz cappilaries were silanized in order to gain hydrophobic properties.

In order to generate stable droplet flow in microfluidic system, a surfactant must be used. Moreover, the surfactant should not interact with the protein inside the droplet and denaturate it. In order to validate our SAXS-microfluidic setup and define the best surfactant for droplets generation that will not destabilize proteins, an active and native tetrameric form of rasburicase was tested in droplets with Tris buffer at pH=8.0. 2 wt% perfluororooctanol (PFO) was used as surfactant in Krytox GPL100 oil.

The corresponding SAXS curves of rasburicase describing the scattered intensity as a function of the scattering vector are presented in Figure 4. The black dots correspond to our experimental results whereas the green and

red curves are the scattering intensities obtained from atomic coordinates with CRYSOL for the tetramer and the dimer of rasburicase (1r51.pdb) respectively. The blue curve obtained with OLIGOMER represents the best fit of experimental result and indicates that the protein solution in the droplet is a mixture of 58% tetramer and 42% dimer. Under these experimental conditions (oil and surfactant), rasburicase is a mixture of native tetrameric forms and incompletely dissociated dimeric forms. It suggests that the surfactant at the interface, in particular the surfactant polar heads in the aqueous droplet may interact with tetramers of rasburicase, dissociating tetramers into dimers. In conclusion, the perfluoorooctanol can denaturate proteins which seriously limits its use in microfluidic experiments.

To avoid denaturation and interaction of surfactant with proteins in droplets, a biocompatible surfactant was synthetized. A tri-block copolymer PFPE-PEG-PFPE described elsewhere was used at concentration of 2 wt% in Krytox GPL100. SAXS experiment with rasburicase is presented in the Figure 4. With this surfactant, it appears that the CRYSOL curve for the tetramer of rasburicase perfectly fits our experimental data, proving that the protein is not denaturated/dissociated meaning that the surfactant is inert with respect to the protein.

Moreover, this shows that using our microfluidic set-up, experimental SAXS data that are in good agreement with crystallographic structures of macromolecules in solution can be obtained. PFPE-PEG-PFPE and Krytox GPL100 appear to be the right combination of compounds to study protein structure in droplets as macromolecules behave exactly as in usual SAXS experiments in microvolumes.

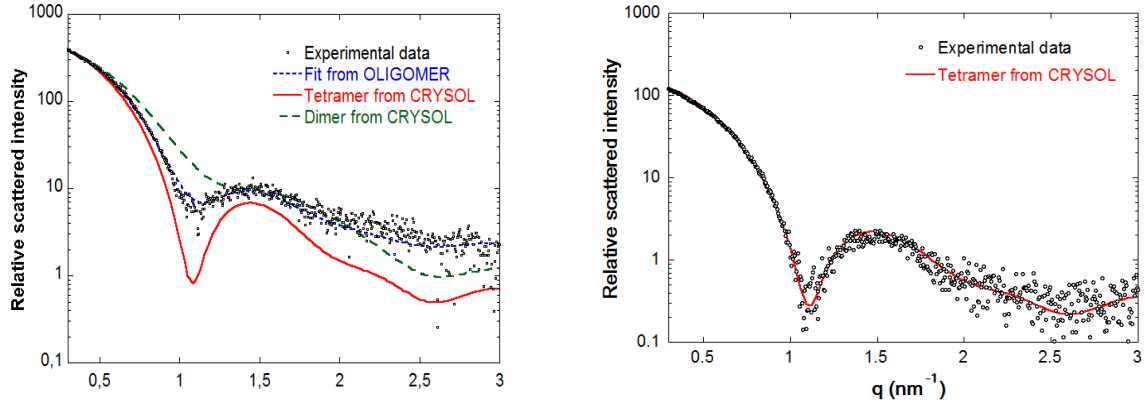

Figure 4- SAXS curves of rasburicase with PFO surfactant (Top) SAXS curve of rasburicase with PFPE-PEG-PFPE surfac-tant (Bottom). Blacks dots are experimental data, green and red curves are scattering curves from atomic coordi-nates for tetramers (1r51.pdb) and dimers respectively, blue curve is the best fit for mixture of dimers and tetramers.

YEAR 2:

The first part of the second year 2 is dedicated to SAXS experiments to elucidate protein phase diagram and molecular interactions in solution and to follow in-situ crystal growth of Glucise isomerase

Objectives: *The main objective of this task is first to test the microfluidic chips for protein crystallization and to get 1/information on protein structure and molecular interactions in solution and 2/ the size distribution of the primary particle in solution.*

Microfluidic chips and suitable oil and surfactant found during first year have been used to study two other proteins: glucose isomerase and lysozyme. We study the crystallization of glucose isomerase induced by a depletion mechanism by adding a surfactant (forming huge micelles in solution). Micelles can act on proteins in the crystallization process as polyethylene glycol, i.e. by a depletion mechanism, putting proteins closer to each other which lead to crystallization.

a/ Online analysis of Glucose Isomerase crystal Growth

The advantage of the current microfluidic set-up is to quickly screen different experimental conditions just by changing flow rates of stock solutions. The conditions used are summarized in Table 3. The photograph of

droplet generation is shown in Figure 5. Small crystals appear just after the droplet generation which is caused by a phase transition within droplets. The SAXS curves of glucose isomerase crystallization are shown in Figure 6.

At lower scattering vectors ($q < 0.5$ nm^{-1}), when the concentration of surfactant increases, it is observed that the scattered intensity is lowered, meaning that the concentration of protein in solution is reduced. On the other hand, at higher scattering vectors ($q > 0.5$ nm^{-1}), when the concentration of surfactant is increased, diffraction peaks appear and get higher and narrower.

Table 1: Flow rates of the stock solutions and concentrations of the different compounds in the droplets

Flow Rates (µL/min)				Concentrations	
Oil	Glucose Isomerase	Surfactant	Buffer MES	GI (mg/mL)	Surfactant (wt %)
2	0.7	0.4	1.5	13.5	0.6
2	0.7	0.6	1.3	13.5	0.9
2	0.7	1	0.9	13.5	1.5
2	0.7	1.2	0.7	13.5	1.8
2	0.7	1.4	0.5	13.5	2.2

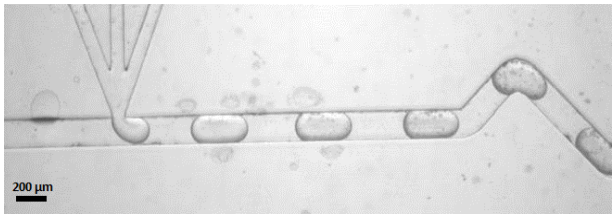

Figure 5- Photograph of the droplet generation during the phase transition experiments. Left channel contains the oil with surfactant, top left channel the crystallization agent, top middle channel the buffer and top right channel the protein. Crystal appearance within the droplets after their formation indicating the existence of a phase transition.

The diffraction peaks indicate the presence of crystals. By increasing the concentration of surfactant, the glucose isomerase undergoes a phase transition from a liquid to a solid crystal phase. With more surfactant, more depletion appears and the crystallization is easier. Consequently, less protein is present in solution (lower SAXS intensity) and bigger crystals (higher and narrower peaks) are created.

Thanks to the known crystal structure parameters of the glucose isomerase, indexation of diffraction peaks is possible. The indexes found fit perfectly with the scattering vectors of the diffraction peaks, proving that the crystals within the droplets are really glucose isomerase crystals.

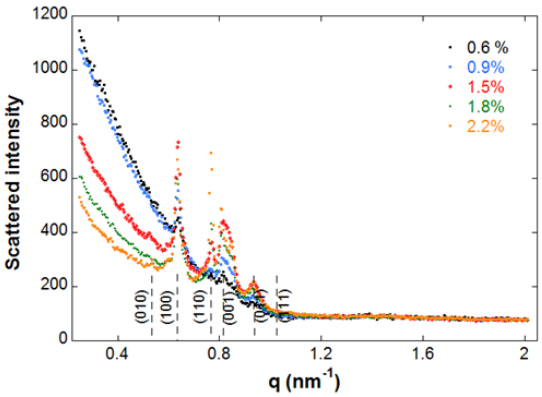

Figure 6- SAXS curves of glucose isomerase with increasing crystallization surfactant concentration.

This experiment clearly demonstrates that a liquid-solid phase transition can be obtained within the droplets using our experimental set-up. Moreover, this set-up has been continuously used for a prolonged period of several hours and no radiation damage or fouling has been observed on the capillary.

b/ A fast and efficient way for measuring protein-protein interactions

In addition, during the first part of the second year, the protein-protein interactions were also studied. Lysozyme was used as a model protein. The experiment was carried out using lysozyme at a stock concentration of 130 mg/mL in sodium acetate buffer at pH=4.4. NaCl was used as crystallizing agent at a stock concentration of 2M, and the continuous phase was formulated according to the previous validation experiment thus ensuring no interaction between protein and droplet interfaces. Figure 7 shows a picture of the microfluidic platform in operation. The continuous phase (oil) is injected in the left channel, salt in the top left channel, buffer in the top middle channel and protein in the top right channel, respectively.

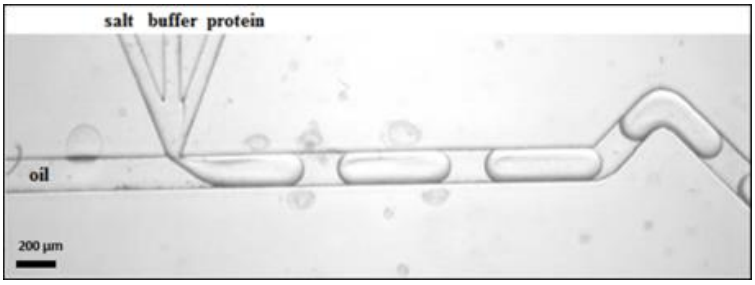

Figure 7- Screen snapshot of droplet generation recorded during crystallization experiments for interaction screening. Left channel contains the oil with surfactant, top left channel the salt, top middle channel the buffer and top right channel the protein.

Interactions can be characterized by a second virial coefficient A_2, which corresponds to variations of S(c,q=0) as a function of macromolecule concentration.

$$S(c, q = 0) = \frac{1}{1 + 2MA_2c}$$

A_2 is the second virial coefficient, M is the molecular weight of the macromolecules and c is their concentration. When S(c,q=0) <1 (respectively, >1), macromolecules are under repulsive interactions (respectively, attractive interactions). Therefore if A_2 >0 (respectively, <0) macromolecules are in repulsive (respectively, attractive) regime. The second virial coefficient A_2 can be obtained for the different salt concentrations from experimental SAXS data. For a given SAXS curve with fixed protein and salt concentration, the forward intensity I(c,q=0) is obtained when the scattering vector tends to zero from the Guinier plot Ln I(c,q) = f(q2). In the plot S(c,q=0) as a function of the protein concentration c, the slope equals -2MA2 giving access to the value of the second virial coefficient A_2 for each salt concentrations. Typical scattering curves obtained for lysozyme at different NaCl concentrations are presented in Figure 8(a). A_2 values obtained from this work and from literature are plotted in Figure 8(b) as function of salt concentration. This figure shows that a good agreement is obtained between our data and literature data.

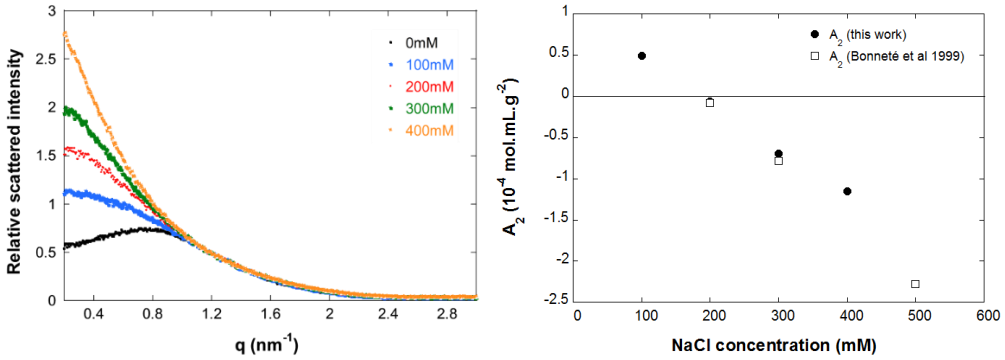

(a) *(b)*

Figure 8- (a) SAXS curves of lysozyme with increasing salt concentration. (b) Variations of second virial coefficient of lysozyme as a function of salt concentration (current study and litterature)

These results show that the **second objective of the year has been accomplished**, our microfluidic set-up coupled to SAXS can be used to have information on protein molecular interactions in solution and protein phase diagram can be elucidated through study of the second virial coefficient.

Objective N°2:

Optimization of the experimental setup: Synchronization between droplets and the X-ray beam.

In order to get a better resolution to be able to catch more subtle features of the nucleation process (i.e. critical nucleus or reversible aggregates responsible of the formation of the first nuclei), it was necessary to improve the measurement process. In addition, this approach will allow to collect unambiguous SAXS data on the solution structure inside the droplets by avoiding the measurement of the signal of the continuous phase (oil) or of the droplet interface. The scheme of the synchronisation setup is given on figure 9.

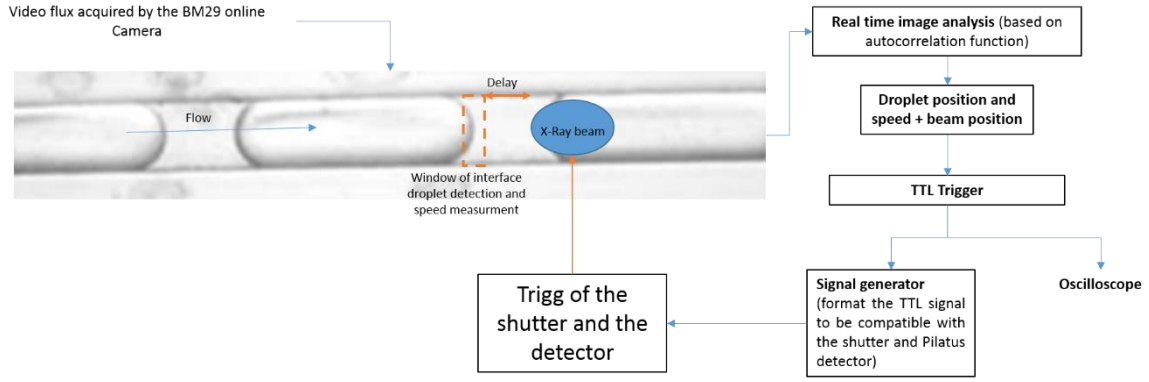

Figure 9- Scheme of the synchronization process: Once the droplets are detected, knowing the speed of each droplet, the beam position and the distance between the window of detection and the beam position, a delay time is calculated (compatible with the opening and closing time of the shutter) and the acquisition is triggered. This approach allows us to get only the SAXS data inside the droplets.

Synchronization is based on a real time image analysis software developed in Matlab and Python (for a better integration in BM29 software environment), using OPEN CV library.

The second part of the second year 2 was dedicated to time-resolved SAXS experiments to have information on first clusters of nucleation.
Objectives: *The main objective of this task was to store droplets in a chip, induce crystallization conditions by cooling down the system and send the droplets to the beam with different time intervals to see the evolution over the time and try to observe clues of the first nuclei.*

Using the microfluidic design shown in figures 10 and 12, droplets of identical operating conditions (temperature, concentration and volume) have been continuously generated in a microfluidic device outside the SAXS sample chamber. The droplet has been stored at a given temperature either in a reservoir (fig. 10) or in the serpentine (fig. 12). After a given time of incubation, the droplets are sent to the sample exposure unit. For maximum flexibility, the residence time of the droplets inside the sample exposure unit can also be adjusted by tuning flow rate of the continuous phase.

For the run of **February 2015**, we used chips with the design presented as below in figure 11. The droplet are generated in a W junction for the 3 aqueous phases containing lysozyme, acetate buffer, and a solution of $NaNO_3$ salt used as crystallization agent. Droplets were generated and then instead of being directly sent to the beam, they were stocked in storage zones. It was then possible to send the droplets to the beam at different time intervals.

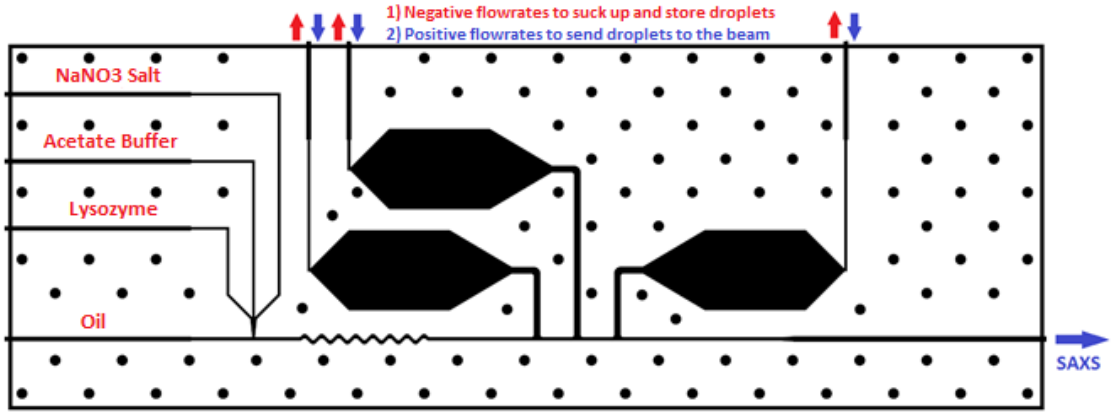

Figure 10- Design for the chip used for time-resolved SAXS

Thanks to Peltier elements attached to the chip, droplets were generated at a temperature of 45°C to avoid local supersaturation that could induce precipitation in the chip and flow rates were set to have a final concentration of 40mg/mL for lysozyme and 400mM for $NaNO_3$ in the droplets. Approximately 300 droplets were stored, then flow rates were stopped and the chip was cooled down to 25°C to induce supersaturation. Droplets were then sent to the beam every 5 minutes.

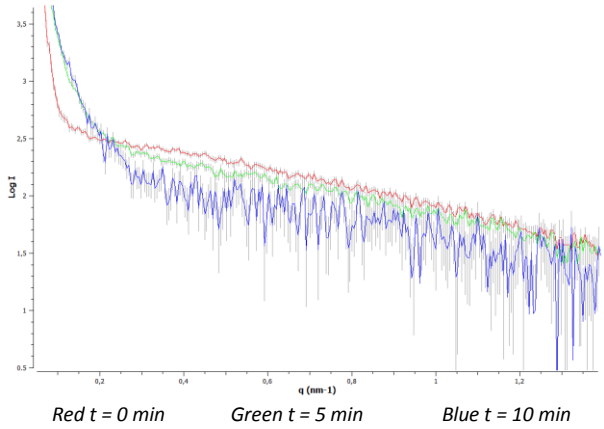

Figure 11- SAXS curves of lysozyme with increasing time of storage in the chip

Corresponding SAXS curves are presented in figure 4 above. It turns out that when time increases, the monomer of lysozyme in solution is consumed (decrease of the signal at high angles) and bigger objects are formed (increase of the signal at small angles). For longer times, the chip started to clog and the protein started to stick and agglutinate in the chip.

No other results could be obtained because of a large waste of time (1 day) due to the shutter synchronization problem discussed above. These results were obtained unplugging the shutter and exposing the oil.

YEAR 3

STUDY OF LYZOZYME NUCLEATION

In the run of **October 2015** a new design was used for the chip to prevent the clogging of the chip. The droplet generation is still the same with a junction for the 3 aqueous phases containing lysozyme, acetate buffer, and NaCl salt for this time. This time, droplets are stocked in a serpentine.

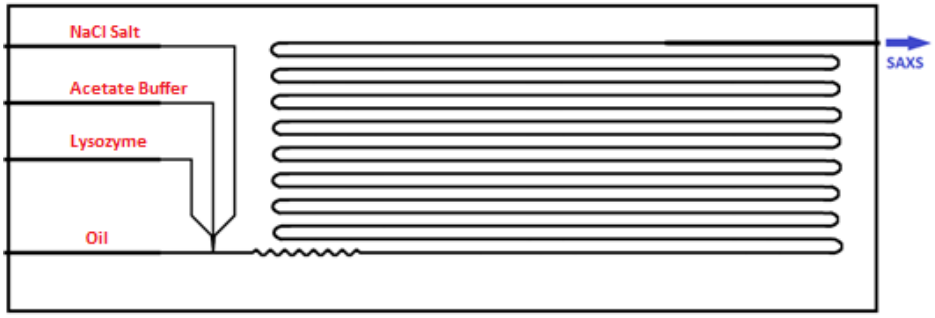

Figure 12: New design of the chip for time-resolved SAXS

This time, droplets were generated at 40°C for the storage and the concentrations in the droplets were 125 mg/mL for lysozyme and 750 mM for NaCl. Once the storage is finished, the chip is cooled down to 25°C. In these operating conditions, the lysozyme is close to the liquid-liquid phase separation as illustrated in the phase diagram presented in figure 13.

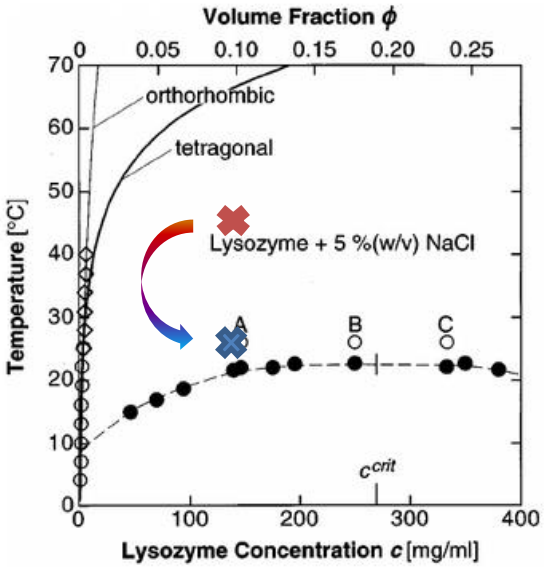

Figure 13: Phase diagram of lysozyme (dashed line = liquid-liquid phase separation)

With such experimental conditions, one can expect a fast nucleation of a lot of small crystals. Droplets have been stored for 1 hour in the storage serpentine then sent to the beam. The average SAXS signal obtained is presented in the figure 14.

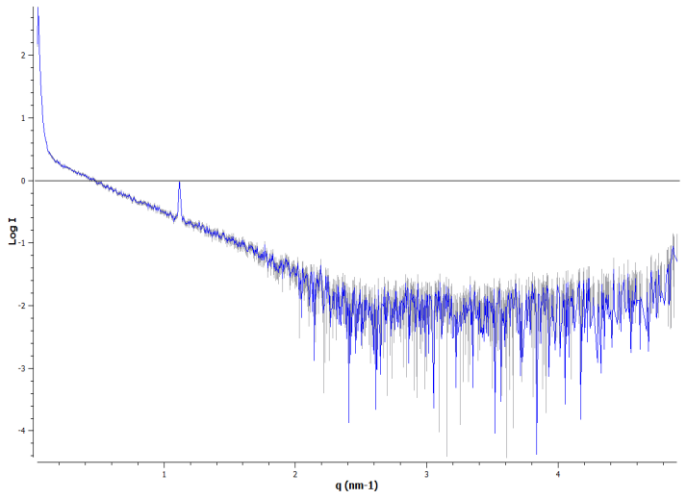

Figure 14 - Average SAXS signal of droplets stored for 1 hour

A diffraction peak appeared on all the frames illustrating the fact that crystals were present in all the droplets. This means that the storage time is too long to see precursors of nucleation.

For the second experiment, storage time was reduced to 10 min to observe what happens before crystallization. Two types of curves were then obtained for the droplets sent to the beam and are presented in figure 15.

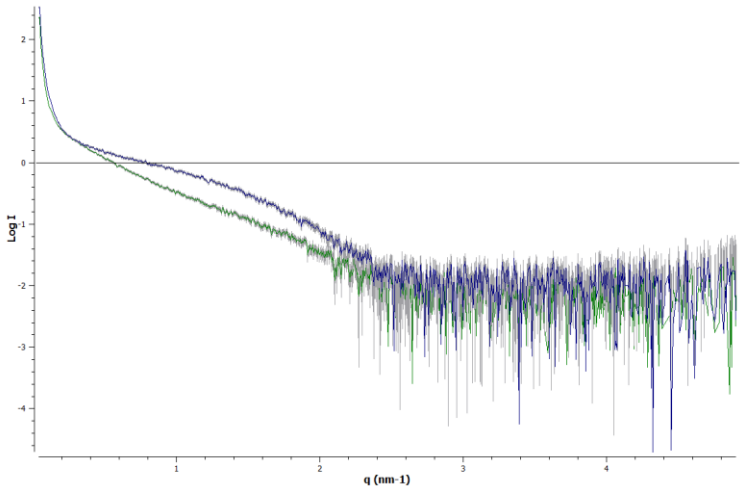

Figure 15- Two types of averaged SAXS curves for droplets stored 10 minutes in the chip.

For most of the droplets (around 100) the classical curve of lysozyme in solution is obtained (green curve). But for some droplets (around 10), another kind of curve presenting a broad peak is obtained. This new type of curve could possibly be the signature of the first nuclei appearing before crystallization.

Once again, there were still some problems for the synchronization shutter/beam/droplets in this experiment but some encouraging results in the research of first clusters of nucleation were obtained.

2016/II For the last run of this long term project, we would like to optimize the experimental condition in order to obtain information about nucleation mechanism of lysozyme. To do so, and after discussion with the beam line scientists, we decide to implement on-chip concentration measurement (photonic lab-on-chip, PhLoc) to be sure that the concentration imposed by the different flow rates were the actual concentration inside droplets.

The operation of the PhLoC platform contemplates the injection of up to 3 different aqueous solutions (A, B and C in figure 1b inset) and an inert and immiscible continuous (Krytox GPL 100) phase with surfactant (1% of PFPE-PEG-PFPE) to generate droplets. Reagent solutions (protein solution and buffer) were injected into the PhLoC at controlled flow rates by means of high precision syringe pumps (neMESYS Cetoni, Germany) coupled to 1mL syringes (Hamilton, USA). Different flow rates ratios provide droplets with different protein concentrations. After generation, droplets are quickly homogenised by means of a passive zigzag mixer, and spectrophotometrically monitored (Figure 16-1) before and after droplets storage for tempering into the PhLoC serpentine channel (Figure 16-2). For this purpose, optical interrogation areas were located perpendicularly to the microfluidic channel. The coupling of light to the microfluidic structure was achieved by means of pig tailed 240 µm fiber optics (Thorlabs, USA, NA = 0.22). Self-alignment elements were designed for fiber optics accurate positioning enabling an optimal light coupling-decoupling to the system. A 5 W halogen AvaLight-D(H)-S light source and an Avaspec 2048-USB2 spectrometer (Avantes, Netherlands) were used for light coupling and subsequent spectrum analysis, and absorbance measurements were performed at λ= 280 nm to determine protein concentration. In order to obtain a spectrophotometric time-resolution allowing a correct monitoring of droplets in movement into the PhLoC microfluidic channels, spectra were collected at the shortest possible integration times. For a precise control on macromolecule saturation state in the droplets, the PhLoC platform is held in a Peltier-based thermostated plate. The PhLoC integrates lateral openings for temperature probes insertion (Figure 1b-3) controlling the temperature in the thermostated plate within the range from 0 to 50 ºC. Link between the PhLoC platform and the SAXS sample holder were made by connecting a flexible fused silica capillary (ID 280 µm, OD 360 µm, Postnova analytics) directly to the exit of the microfluidic platform and to the quartz capillary (OD 300µm, wall thickness 10µm) of the sample holder. Temperature was also maintained constant along the connecting capillary by means of a thermostated bath and external tubing surrounding the capillary.

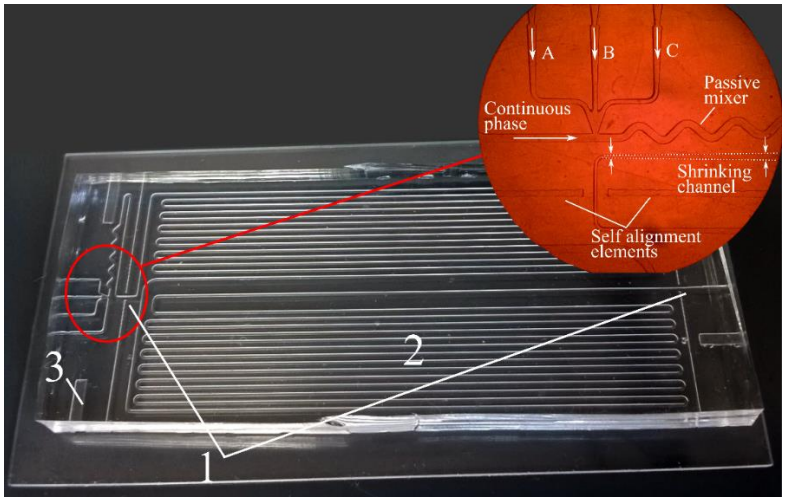

Figure 16- Picture and details of the PhLoC platform showing 1) Interrogation areas for photonic detection, comprising two self-alignment elements for pig-tailed fiber optics positioning, 2) serpentine channel for droplet storage and 3) inlets for temperature probes. Inset show details of the mixing and droplet generation area, comprising 3 channels for reagent injection (A, B, C), an extra channel for continuous phase injection, and a passive zigzag mixer allowing effective and fast droplet homogenisation.

Figure 17a shows the typical intensity spectrum collected when a solution containing NaAc 50 mM buffer pH 4.5 (reference blank for lysozyme absorbance measurements measured at λ= 280 nm) was injected generating monodisperse droplets with the continuous immiscible phase. In this spectrum we can observe both continuous and aqueous phase giving a very constant intensity values (measured at the center of the droplets), and also maximum and minimum light intensity peaks due to light beam interaction with the meniscus corresponding to the aqueous/oil interface. Additionally, it is also possible to observe the droplets as a function of time, obtaining a good measurement of droplet size (once flow rates are determined and fixed) and droplet generation frequency. Moreover, the stability of this pattern described by the intensity spectra allows to

discriminate when droplets generation is unstable (mainly when flow rates are not stabilized) or when droplets are steadily generated (Figure 17b), thus leading to homogenous droplets, which population number and concentration can be straightforwardly determined. According to the protein concentration range to be measured, it becomes necessary to consider a minimum optical path ensuring enough sensitivity. But additionally, in accordance to Lambert-Beer law, when decreasing the optical path, absorbance signal is also decreased, and thus it is also possible to extend the absorbance linear range at higher concentrations. Hence, for the work here presented, in which protein interactions for lysozyme at mid to high concentrations were explored, PhLoCs with two different optical paths for droplet interrogation were considered. One PhLoC was designed with a constant channel width of 280 µm, while a second one was provided by a channel gradually shrinking to reach an interrogation optical path of 150 µm (inset in Figure 16b). Figure 17c shows 2 calibration plots for lysozyme using these two PhLoC configurations. Each absorbance point in this plot represents an average of 20 droplets, showing a very high reproducibility, with a standard deviation of ~ 0.001 absorbance units. As it can be observed, a decrease in the optical paths provides a decrease in the absorbance signal for the same measured concentrations with a consequent extension in the linear range.

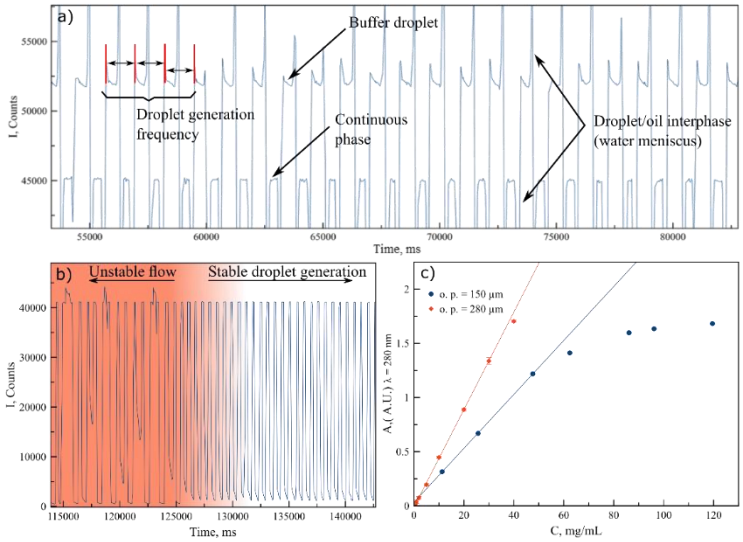

Figure 17- (a) Typical intensity spectra collected at λ= 280 nm when operating with the PhLoC generating stable droplets at constant flow rates. The continuous phase is observed at a constant intensity value while the dispersed aqueous phase can present different intensity values as a function of protein absorbance at the given wavelength; (b) Intensity spectra resulting from monitoring the first instants of droplet generation. Left part shaded in red shows the spectra of different unsteady droplets, leading to different intensity signals at λ= 280 nm, in accordance to their protein concentration. Right part shows steady droplet generation with homogeneous and reproducible protein concentration; (c) Absorbance calibration plots at λ= 280 nm for lysozyme measured on chip through a 150 µm (red squares) and a 280 µm (blue circles) optical paths. Lines depict the concentration linear range for each plot.

Figure 18 shows the intensity curves, $I(c,\vec{q})$, measured as a function of the scattering vector obtained in nano-droplets for different lysozyme concentrations, spectrophotometrically determined on-chip prior to the SAXS measurements. Considering the buffer signal as a background for subtraction and scaling on the same relative value by normalizing the intensity curves as a function of their corresponding protein concentration, c, and direct beam intensity, we can determine the form factor of the protein using the intensity curves recorded at the lowest concentrations.

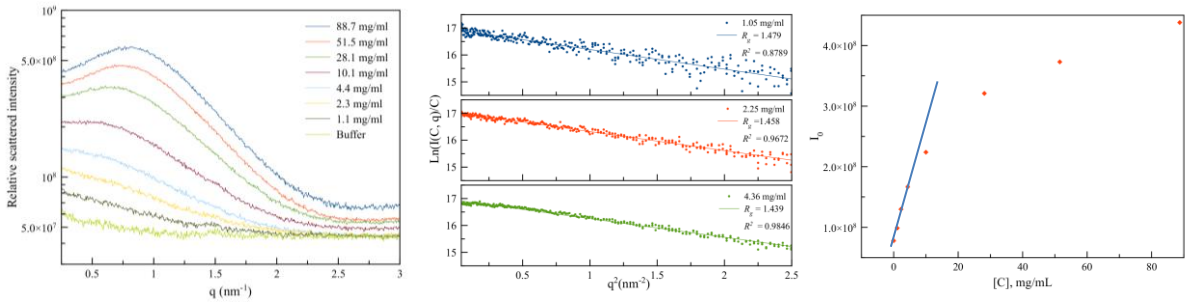

Fig 18 (a)Normalized scattered intensity of lysozyme in NaAC 50mM buffer pH 4.5 at different concentrations. b) Guinier cuvres obtained for different protein concentrations (ranging from 1 to 4.36mg/ml) (c) Evolution of extrapolated Intensity at 0 angle as function of concentration (first part of the curve show a linear range as expected for dilute protein concentration)

The combination of Small-Angle X-Ray Scattering (SAXS), spectrophotometric detection techniques and high throughput, droplet based microfluidics is here proposed as a powerful and versatile tool to investigate protein form factor, protein structure factor and macromolecular interactions. A PhLoC platform was designed for droplet generation, allowing the monitoring of protein concentration in each monodisperse droplet as well as droplet generation frequency. The droplet flow was synchronised to perform synchrotron radiation SAXS measurements in individual droplets, each one acting as an isolated microreactor.

In the second part of the beam time, nucleation experiments were performed using the same microfluidic platform. In these experiments three proteins concentrations have been tested (C=60 – 80 and 110mg/ml) with 5mM sodium acetate as buffer (pH = 4.5) and a salt (NaCl) concentration fixed at 500mM.

In these experiments, 200 droplets were generated and store on chip at 38°C, to avoid unwanted protein precipitation. Then all the droplets are sent to the SAXS exposing unit. The capillary (making the connection between the SAXS sample holder and the chip) was maintained at a constant temperature (10°C). By changing the oil flow rate (from 20µl/min to 1µl/min) different residence times of the droplets inside the cold capillary can be screened. As it is a continuous process, all the droplets have exactly the same residence time inside the cold capillary. This methodology allows us to screen timing (from 30s to 1 hours) after the solution quenching, and thus give us the opportunity to perform time resolved SAXS experiments. When all the droplets were exposed to the X-ray beam, the chip is refilled with another 200 droplets and the oil flow rate is increase to explore another timing. This experiment is repeated until the emergence of crystal in all the droplets.

Typical results obtained at low concentration of proteins (i.e. C<100mg/ml) are presented in figure XX. In these experiments, no special feature (expect interactions between proteins) on the scattering curves has been observed prior to nucleation.

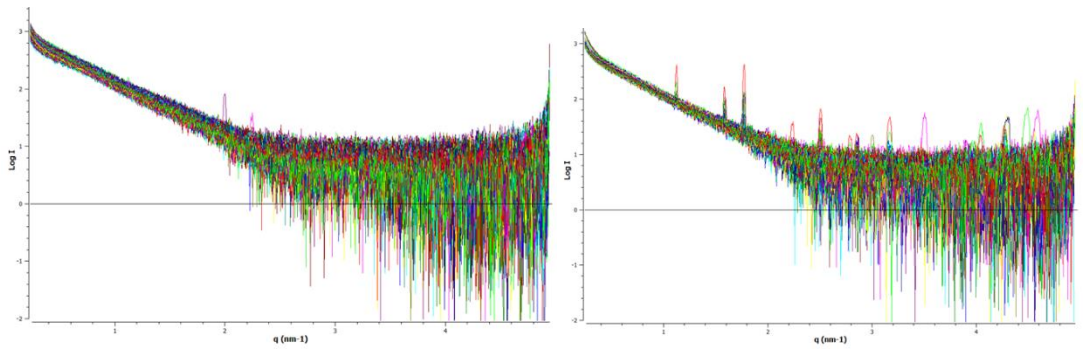

Figure 19 Typical SAXS curve obtained for low supersaturation (C<100mg/ml). (a) for t<10 min (b) for t >20. This figure show the appearance of Bragg peaks in most of the droplets.

However, when the protein concentration is high (C=110mg/ml) ,a very interesting features has been observed in several droplets. As shown in figure 20 (a), different scattering curves have been observed for the same protein and salt concentration. Broad and large peak are obtained with a maximum at q=1.6nm^{-1} and q=0.5nm^{-1} prior to crystal nucleation. In addition, after crystallization the broad peaks disappears, and Bragg peak are observed. Consequently the peak observed prior to nucleation might be a signature of pre-nucleation clusters. Because it is not possible to measure scattering curves at lower angles, the Guinier plateau cannot be observed, and the size of these cluster cannot be determined. However, this result was not expected at the beginning of the project, but it is possible to state that these objects are greater than 25nm (given the q range accessible on BM29).

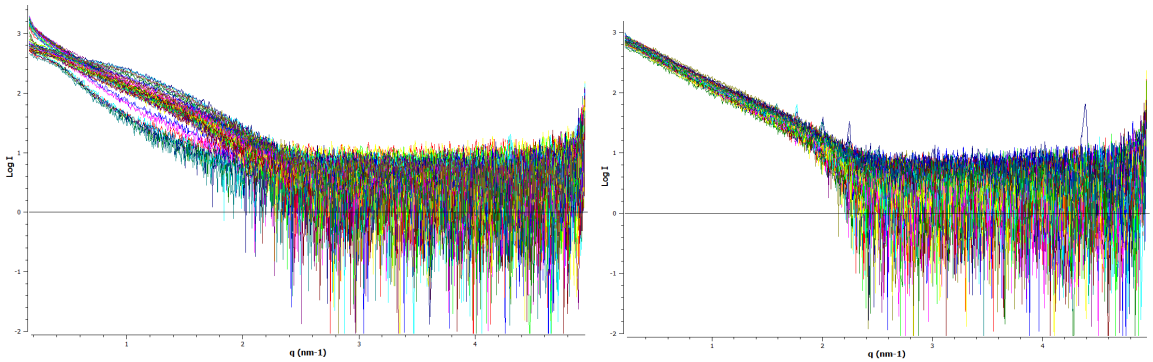

Figure 20- Typical SAXS curve obtained for high supersaturation (C=110mg/ml). (a) for t=6min, this figure show the appearance of a broad peaks, which might be the signature of pre-nucleation clusters. (b) For t >20. This figure show the appearance of Bragg peaks in most of the droplets.

REMARK: The same experiments have been performed in another beamline, with a larger sample to detector distance and the same results were obtained (i.e. a broad peak around 1.6nm^{-1}) and a Guinier plateau is observed corresponding to a cluster size of 60nm. These results will be presented at IuCr meeting and ISIC 20, and a paper is currently being written.

Assessment of support given and received:

This LTP project has been on a strong collaboration established between biophysicists (IBMM Avignon) and chemical engineers (LGC Toulouse) with beamline scientists from ERSF and EMBL who are interested in developing microfluidics for biological macromolecule studies. The success of this project relies on a close collaboration between each partner. During these three years, we share not only scientific and technologic knowledge but also some funding and equipment obtained from other proposals. However much of equipment must be moved from Toulouse to Grenoble during each experiment.

In this project we have developed versatile and robust microfluidic platforms and reliable protocols that can be used for the scientific community and directly applied for other biological system of interest. All the software, chip, design protocols are (or will be) available for the BM29 users who want to use or test microfluidic for their own systems.

To perpetuate this set-up on the beamline for future collaborations, the purchase of 4 to 5 syringe pumps dedicated to BM29 should be considered. In addition, if we want to directly make the measurement inside the microfluidic chips (by placing the chips directly in the sample chamber) some more equipment are needed:

- An in-line camera: to precisely monitor the position of the beam during the measurement.
- A high precision motorized X-Y stage: to map the entire microfluidic chip.

We are convinced that this improvement will be benefit to our study but also to the scientific community since more versatile chips can be tested and all the development performed during this project are available in BM29

beamline. We are convinced that if the sample environments of BM29 can be modified to perfectly fits with microfluidic experiments (by adding syringe pumps, small microscope, spectrometer and light source) the developed microfluidic platform can be a new and more efficient sample delivery system that allows for automatic experiments with a higher throughput experiments, with much lower product consumption (10 order of magnitude less) and more statistically reproducible experiments.